Indian Journal of Chemistry
Vol. 55A, April 2016, pp. 413-422

Experimental and theoretical spectral investigations of 5-chloro-*ortho*-methoxyaniline using FT-IR, FT-Raman and DFT analysis

G Venkatesh[a], M Govindaraju[b,] * & P Vennila[c]

[a]R&D Centre, Bharathiar University, Coimbatore 641 046, India
[b]Department of Chemistry, Arignar Anna Government Arts College, Namakkal 638 052, India
[c]Department of Chemistry, Thiruvalluvar Government Arts College, Rasipuram 637 401, India
Email: kvchempro@gmail.com

Received 17 September 2015; re-revised and accepted 28 March 2016

Vibrational spectral analyses have been carried out using FT-IR and FT-Raman spectra for 5-chloro-*ortho*-methoxyaniline (5COMA). The fundamental vibrational frequencies and intensity of vibrational bands are evaluated using density functional theory. The vibrational spectra have been interpreted with the help of normal coordinate analysis based on scaled quantum mechanical force fields. The first-order hyperpolarizability and the anisotropy polarizability invariant have been computed with the numerical derivative of the dipole moment. The HOMO-LUMO energies, atomic charges, hardness, softness, ionization potential, electronegativity and electrophilicity index have been calculated. Natural atomic charges, nonlinear optical, ^{1}H NMR and ^{13}C NMR data have been employed to study the electronic properties of 5COMA using the B3LYP functional with 6-311G** basis set. Molecular electronic potential and Mulliken's charges have been obtained using the DFT calculation method. Electronic excitation energies, oscillator strength and nature of the respective excited states have been calculated by the closed-shell singlet calculation method.

Keywords: Theoretical chemistry, Density functional calculations, Natural atomic charges, Nonlinear optics, Vibrational spectroscopy, Raman spectroscopy, HOMO-LUMO, First-order hyperpolarizability

The discovery of new drugs requires molecular modelling which significantly contributes in the prediction of molecular properties. 5COMA (also known as 5-chloro-*o*-anisidine) is an aniline derivative, with amino and methoxy functionals which are strong and weak activating groups, respectively. 5COMA functions as an intermediate in several organic reactions since it has highly active nitrogen where nucleophilic aromatic substitution or electrophilic substitution can occur[1]. The synthesis of dyestuffs, pigments, pesticides and other organic chemicals involve the formation of intermediates of aniline derivatives. These derivatives are hazardous, toxic and harmful for the environment. Aniline derivatives find importance in synthesis of local anesthetics due to the interaction of amino group with the receptor[2]. Thus, the investigation of molecular properties and nature of chemical reaction mechanism they undergo, has received much attention in the field of drug delivery. The enhanced interaction of the amino group with aromatic ring in aniline derivatives implied the change in molecular geometry[3]. Hence, the study of relationship between the molecular geometry and vibrations of derivatives of aniline has been widely studied in the recent past.

Kolandaivel *et al.*[4] have been reported the DFT (B3LYP) calculation of m-anisidine. The FT-IR, FT-Raman, NMR spectra and DFT calculations of 4-chloro-N-methylaniline has been studied by Usha Rani and co-workers[5]. Karabacak *et al.*[6] examined the FT-IR, FT-Raman, NMR spectra and DFT calculations of 2-chloro-N-methylaniline. Further, Sivaranjini *et al.*[3] reported the vibrational and theoretical evaluation of 3-methoxyaniline. The FT-IR, FT-Raman and DFT calculations of 2-chloro-5-methylaniline and 2-chloro-4-methylanilne were reported by Karabacak and co-workers[7, 8]. From the literature, it is clear that, various aniline derivatives have been examined for their structural features and spectral assessments. In a continuation to study the properties of aniline derivatives, herein the FT-IR, FT-Raman, NMR, NLO, MEP and NBO analyses of 5COMA have been carried out by DFT calculations using B3LYP/6-311+G** functional.

Materials and Methods

Experimental details

The 5COMA of spectroscopic grade compound was purchased from Lancaster Chemical Company,

UK. FT-IR spectra of 5COMA were recorded in the region 4000–400 cm^{-1}, at a resolution of ±1 cm^{-1}, 16 scan number using Bruker IFS 66V vacuum FT spectrometer with a KBr beam splitter and Globar source. The FT-Raman spectra were also recorded on the same instrument with FRA 106 Raman accessories in the region 4000–100 cm^{-1}. Nd:YAG laser operating at 200mW power with 1064 nm excitation was used as light source.

Computational details

The quantum chemical calculations were carried out by applying DFT method and using GAUSSIAN 09W program B3LYP functional supplemented with the standard 6–311+G** basis set[9-11]. The theoretical force constants in Cartesian representation have been computed at the completely optimized geometry. The potential energy distribution (PED) and normal coordinate analysis were carried out by MOLVIB program by Sundius. The Raman activities (Si) calculated by the GAUSSIAN 09W program with help of the MOLVIB were transformed to relative Raman intensities (Ii) using the following relationship derived from the fundamental theory of Raman scattering[12, 13].

$$I_i = \frac{f(v_0 - v_i)^4 Si}{v_i[1 - exp(-hcv / KT)} \quad \ldots(1)$$

Here, υ_0 represents exciting frequency (in cm^{-1}), υ_i represents the vibrational wave number of the normal mode; h, c and k are universal constants, f is normalization factor.

NOB analysis gives information about the charge transfer or conjugative interaction of the entire molecular system. Electron donor orbital, electron acceptor orbital and the interacting stabilization energy of a molecule can be explained by second-order micro-disturbance theory[14, 15]. The higher E(2) values observed indicate an intensive interaction of donor orbital and acceptor orbital of the whole system[16]. The second order Fock matrix employs donor (i) acceptor (j). For each donor (i) and acceptor (j), the stabilization energy $E(2)$ associated with the delocalization, i to j was calculated as,

$$E(2) = \Delta E_{ij} = q_i \frac{F(i,j)^2}{(\varepsilon_i - \varepsilon_j)} \quad \ldots(2)$$

where q_i is the donor orbital occupancy, are d_j and d diagonal elements and F(i, j) is the off diagonal NBO Fock matrix element.

Results and Discussion

Molecular geometry

The optimized molecular structure of 5COMA is shown in Fig 1, which has C_s point group of symmetry. The global minimum energy obtained by the DFT structure optimization is presented in Table S1 (Supplementary Data). The optimized structural parameters, viz., bond length, bond angles and dihedral angles were also calculated by DFT with Gaussian 09W package employing B3LYP method. Table 1 comprises the parameters obtained from the molecular geometry of 5CMA. From the table, it is clear that, the molecule has the following bond lengths viz., 1.386 – 1.385 Å for C-C bond, 1.121 Å for ring C-H, 1.22 Å for exocyclic C-H (-OCH_3), 1.409 Å for C-O and 1.476 Å for C-Cl. It can be seen that bond angles of all atoms except exocyclic methoxy carbon are almost equal. This may be attributed to the resonance effect of benzene ring. The decrease in methoxy bond angle compared to other bond angles is resulting from the *ortho* effect. The small discrepancies between calculated and standard values given in literature could be due to the fact that the theoretically calculated values correspond to gaseous phase molecule whereas the values given in literature are for solid phase molecules.

Vibrational spectral analysis

The vibrational assignments of 5COMA are listed in Table 2. The observed and theoretical FT-IR and FT-Raman spectra of 5COMA are shown in Figs 2 and 3. 5COMA includes 48 normal modes of

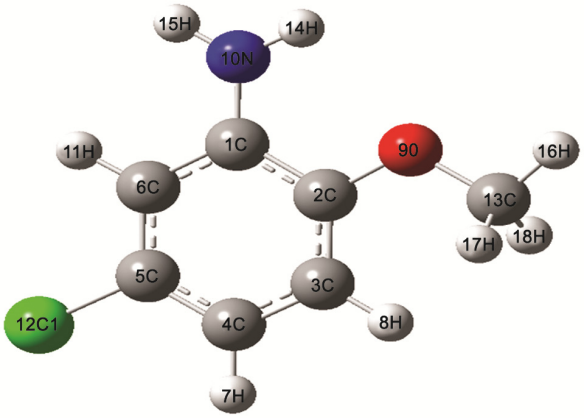

Fig. 1 – Optimized molecular structure of 5COMA.

Table 1 – Optimized geometrical parameters of 5COMA obtained by B3LYP/ 6–311+G**

Bond length[a] (Å)		Bond angle[a] (Å)		Dihedral angle[a] (Å)	
C2-C1	1.4194	C3-C2-C1	120.00163	C4-C3-C2-C1	0.00000
C3-C2	1.3918	C4-C3-C2	120.00023	C5-C4-C3-C2	0.00000
C4-C3	1.4083	C5-C4-C3	120.00023	C6-C1-C2-C3	0.00000
C5-C4	1.3859	C6-C1-C2	119.99816	H7-C6-C1-C2	-179.42805
C6-C1	1.4059	H7-C6-C1	120.00081	H8-C1-C6-C5	179.42805
H7-C6	1.12197	H8-C1-C6	119.99639	O9-C2-C1-C6	179.42754
H8-C1	1.12192	O9-C2-C1	119.99692	N10-C3-C2-C1	-179.42347
O9-C2	1.40995	N10-C3-C2	120.00050	H11-C4-C3-C2	179.42800
N10-C3	1.44594	H11-C4-C3	120.00081	Cl12-C5-C4-C3	179.42864
H11-C4	1.12197	Cl12-C5-C4	119.99899	C13-O9-C2-C1	-59.42661
Cl12-C5	1.76006	C13-O9-C2	109.49987	H14-N10-C3-C2	-0.00376
C13-O9	1.40995	H14-N10-C3	120.00050	H15-N10-C3-C2	-179.42706
H14-N10	1.02803	H15-N10-C3	120.00487	H16-C13-O9-C2	180.00000
H15-N10	1.02796	H16-C13-O9	109.49948	H17-C13-O9-C2	59.93309
H16-C13	1.12204	H17-C13-O9	109.50431	H18-C13-O9-C2	-59.93228
H17-C13	1.12203	H18-C13-O9	109.50283		
H18-C13	1.12201				

[a]for numbering of atom refer to Fig. 1.

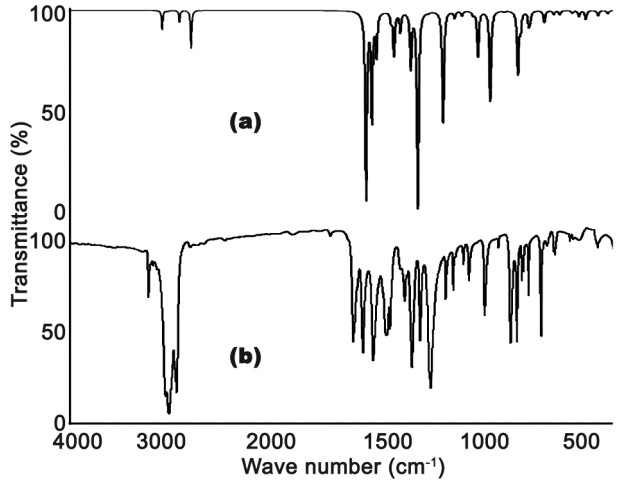

Fig. 2 – The FT-IR spectra of 5COMA. [(a) experimental; (b) theoretical with B3LYP/6-311+G**].

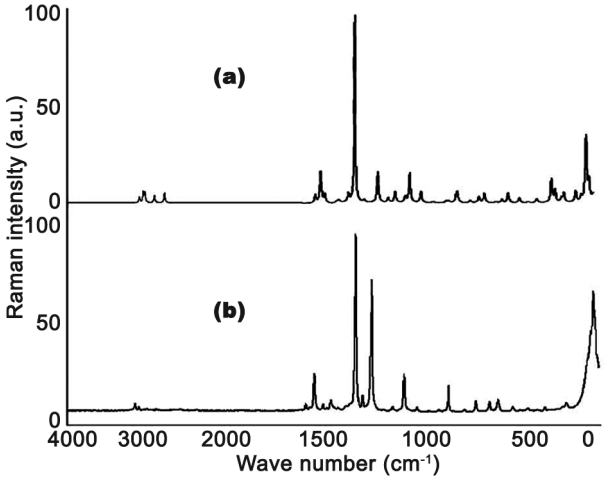

Fig. 3 – The FT-Raman spectra of 5COMA. [(a) experimental; (b) theoretical with B3LYP/6-311+G**].

vibrations, 33 in-plane vibrations and 15 residual out-of-plane vibrations. The 48 normal modes of vibrations were distributed as Γ_{3N-6}= 33 A' (in-plane) + 15 A″ (out-of-plane) and are in agreement with C_s symmetry. The 48 normal modes of vibrations were active both in FT-IR and FT-Raman. The normal coordinate analyses have been discussed to describe the vibrational modes. The full set of 62 standard internal coordinates containing 14 redundancies are listed in Table S2 (Supplementary Data). Fogarasi *et al.*[17-19] reported that linear combinations of internal coordinates were constructed to a non-redundant set of local symmetry coordinates (Table 3). The vibrational coordinates used in all subsequent calculations were transformed by DFT force fields. Root mean square (RMS) values of frequencies were obtained using the following equation,

$$\mathrm{RMS} = \sqrt{\frac{1}{n-1}\sum_{i}^{n}(U_i^{\mathrm{calc}} - U_i^{\mathrm{exp}})^2} \qquad \ldots(3)$$

The RMS error of frequencies (B3LYP/ 6-311+G**) was found to be 110 cm^{-1} for 5COMA. The least square refinement algorithm of RMS deviation was 6.42 cm^{-1}.

Benzene and its derivatives usually show C–H stretching vibrations[20] in the region of 3300–3100 cm^{-1}. The observed and calculated vibrational frequencies are given in Table 2. The FT-IR bands at 3198, 3196,

Table 2 – Detailed assignments of fundamental vibrations and TED of 5COMA

No.	Symmetry species C_s	Observed frequency (cm^{-1})		Calculated frequency (cm^{-1}) with B3LYP/6-311+G** force field				TED (%) among type of internal coordinates[c]
		Infrared	Raman	Unscaled	Scaled	IR[a] A_i	Raman[b] I_i	
1	A'	3677		3675	3672	19.259	58.695	ν NH(100)
2	A'		3570	3569	3568	22.811	165.104	ν NH(100)
3	A'	3245		3242	3240	34.284	102.843	ν CH(99)
4	A'	3212	3216	3215	3211	4.672	131.739	ν CH(99)s
5	A'	3192		3198	3196	10.042	54.699	ν CH(99)
6	A'		3189	3188	3185	5.312	68.230	γ CH_3 (95)
7	A'	3088		3089	3087	54.860	115.808	β CH_3(59), ν CH_3(35), γ CH_3 (5)
8	A'		3030	3029	3028	30.530	71.911	ν CH_3(62), β CH_3 (38)
9	A'	1692		1690	1689	128.152	29.001	bHNH(66), ν CC(16), ν CN(9)
10	A'			1650	1648	6.561	33.245	ν CC(55), bHNH(15), bCH(13), bring(9)
11	A'		1646	1645	1642	4.334	3.989	ν CC(69), bring(10), bCH(6)
12	A'	1565		1562	1559	93.248	7.261	ν CC(37), bCH(36), ν CN(8), ν CO(8), bmsb(5)
13	A'		1542	1539	1537	127.882	8.529	γ CH_3 (87), β CH_3 r(5)
14	A'	1525	1523	1521	1519	5.719	25.891	β CH_3 (59), γ CH_3 (40)
15	A'			1504	1501	21.842	6.363	ν CH_3(86), bCH(5)
16	A'	1476		1475	1472	11.329	1.769	ν CC(46), bCH(22), ν CN(9), bCNH(7)
17	A'		1387	1388	1386	4.045	14.502	ν CC(80), ν CO(6)
18	A'		1338	1329	1326	2.900	0.810	bCH(43), ν CC(18), ν CN(12), bCNH(9), ν CO(5), bCO(5)
19	A'	1322		1320	1318	76.171	7.051	bCH(52), ν CC(20), ν CN(15), ν CO(5)
20	A'		1267	1268	1265	202.817	2.746	ν CO(41) S, ν CC(19), bring(15), ν CN(8)
21	A'	1226		1224	1222	91.383	5.438	β CH_3 r(53), γ CH_3 r(16), ν CO(6), bCH(5)
22	A'		1192	1190	1188	0.776	5.045	γ CH_3r(57), β CH_3 r(18), β CH_3 (14), γ CH_3 (11)
23	A'	1183		1179	1177	17.433	3.074	bCH(54), ν CC(21), bCNH(13), β CH_3r(5)
24	A'		1134	1133	1131	14.051	3.840	ν CC(37), bCH(26), bCNH(20), ν CCl(6)
25	A'	1110		1108	1107	10.199	8.331	ν CC(30), ν CO(25), bCNH(22), bCH(9), ν CCl(8)
26	A'	1073	1067	1071	1069	52.779	4.292	ν CO(50) S, ν CC(20), bring(18), bCNH(5)
27	A'			920	916	22.612	0.914	bring(50), ν CCl(22), ν CN(11), ν CC(7)
28	A"	901	903	905	902	18.324	1.057	gCH(86), tring(12)
29	A"	848		846	844	26.926	2.364	gCH(82), tring(13)
30	A"	797		802	799	29.458	1.789	gCH(76), tring(11), gCO(9)
31	A'		788	782	779	5.696	24.707	ν CC(39), ν CO(22), bring(19), bCO(10)
32	A"	716		712	709	13.941	0.291	tring(61), gCO(14), gCN(10), gCCl(7), gCH(6)
33	A"			660	656	72.676	2.577	gCNH(40), ν CCl(21), bring(9), ν CO(8), ν CC(6), bCO(6)
34	A"	628	630	629	625	236.628	6.989	gCNH(51), bHNH(18), tring(7),ν CN(5)
35	A"			587	585	22.865	2.904	tring(39), gCCl(21), gCO(18), gCN(10)
36	A"	570		569	567	58.357	1.491	gCNH(20), bCO(15), bCN(11), tring(7), ν CN(7), bHNH(7)
37	A'		571	520	516	5.275	3.702	bring(45), bCO(28), ν CN(7), ν CC(5)
38	A"	502		459	457	13.527	0.557	tring(61), gCN(19), gCO(8), gCH(6)
39	A'		403	410	406	1.758	2.200	bCO(23), ν CCl(22), bCN(21), bCCl(11), bring(11), ν CC(7)
40	A"			380	377	3.274	0.522	gCO(25), gCCl(18), gCN(15), tOCH3(13), tring(12), gCH(7)
41	A'		340	339	336	0.914	6.747	bring(36), bCO(17), bCN(16), ν CCl(12), ν CC(7), bCCl(5)
42	A"			336	332	25.646	1.939	tNH2(76)
43	A'		268	265	260	3.749	2.552	bCCl(36), bCN(30), bCO(18), bring(7)
44	A"			260	255	1.229	0.339	tOCH3(76), tring(8)
45	A"		211	210	206	3.954	1.235	tring(40), gCN(21), gCCl(16), gCH(13)
46	A'			208	203	1.557	0.574	bCO(54), bCCl(36), ν CC(7)
47	A"		138	142	139	3.623	0.007	tring(51), tCOm(28), gCCl(9), gCH(8)
48	A"			72	70	1.094	1.094	tCO(61), tOCH_3(27), tring(5)

Abbreviations used: ν, Stretching; β, bending; g, wagging; t, torsion; b, bending; g, wagging; r, rocking.

[a] Relative absorption intensities normalized with highest peak absorption

[b] Relative Raman intensities calculated by Eq. 1 and normalized to 100.

[c] For the notations used, see Table 3.

Table 3 – Local symmetry coordinates and scale factors of 5COMA

No.(i)	Symbol[a]	Definition[b]	Scale factors used in calculations
1-6	C-C	r1,r2,r3,r4,r5,r6	0.914
7-9	C-H	S7,S8,S9	0.914
10-11	C-O	p10, p11	0.992
12	C-N	P12	0.992
13	C-Cl	n13	0.992
14-15	N-H	N14,N15	0.992
16	Mss	(ψ16+ψ17+ψ18)/ √3	0.995
17	Mips	(2ψ17-ψ16-ψ18)/ √6	0.992
18	Mops	(ψ17-ψ18)/ √2	0.919
19	C-C-C	(α19-α20+α21-α22+α23-α24)/ √6	0.992
20	C-C-C	(2α19-α20-α21+2α22-α23-α24)/ √12	0.992
21	C-C-C	(α20-α21+α23-α24)/2	0.992
22-24	C-C-H	(θ25-θ26)/√2, (θ27-θ28)/√2, (θ29θ30)/√2	0.916
25-26	C-C-O	(β31-β32)/√2, β33	0.923
27	C-C-N	(Φ34-Φ35)/√2	0.923
28	C-N-H	(γ36-γ37)/√2	0.990
29	H-N-H	(μ38	0.990
30	C-C-Cl	(ν39- ν40)/√2	0.990
31	Msb	(φ41+φ42+φ43-ι44-ι45-ι46)/ √6	0.990
32	Mipb	(2φ43-φ41-φ42)/ √6	0.990
33	Mopb	(φ41-φ43)/ √2	0.990
34	Mipr	(2ι45-ι44-ι46)/ √6	0.990
35	Mopr	(ι44-ι46)/ √2	0.990
36-38	C-H	ω47, ω48, ω49	0.994
39	C-O	ξ50	0.962
40-41	C-N	Ω51, Ω52	0.962
42	C-Cl	ϖ53	0.962
43	Tring	(τ54-τ55+τ56-τ57+τ58-τ59)/√6	0.994
44	Tring	(τ54-τ56+τ57-τ59)/2	0.994
45	Tring	(-τ54+2τ55-τ56-τ57+2τ58-τ59)/√12	0.994
46	C-O	τ60	0.979
47	C-C-H	τ61/3	0.979
48	N-H	τ62/2	0.979

[a]These symbols are used for description of the normal modes by TED in Table 2.
[b]The internal coordinates used here are defined in Table S2.

3192 cm^{-1} and Raman bands at 3245, 3242, 3240 cm^{-1} are assigned to C–H stretching vibrations. The bands due to C–H bending vibrations of 5COMA appear at 1476, 1475, 1322, 1320, 1318 cm^{-1} in the FT-IR spectrum and at 1338, 1329, 1326 cm^{-1} in the FT-Raman spectrum. The shifting of C-C stretching to lower wave numbers show predominant action of C–H bending vibrations.

Benzene and its derivatives generally show C–C stretching[21] vibrations in the region 1700–1495 cm^{-1}. The C–C bands at 1692, 1565, 1476 cm^{-1} in FT-IR and at 1646, 1645 and 1642 cm^{-1} in the FT-Raman spectra are due to C-C stretching of 5COMA. The bands ascribed at 1183, 1110, 1073 cm^{-1} and 1134, 1133, 1067 cm^{-1} may be designated as the C-C in-plane bending of 5COMA.

The C–N stretching absorptions were observed in the region of 1382–1266 cm^{-1} for aromatic amines[3, 22]. The C-N stretching vibrations were observed in FT-IR spectrum at 1476, 1475, 1322, 1320, 1318 cm^{-1} and in the FT-Raman spectrum at 1338, 1329, 1326, 1267, 1265 cm^{-1}. These two types of deformations include out-of-plane deformations of aromatic ring with in-plane deformations of C-N and in-plane deformation of aromatic ring with out-of-plane deformation of C-N, which is evident from the bands at 502, 459, 457 cm^{-1} in FT-IR and 410, 406 403 cm^{-1} in FT-Raman spectra. The FT-IR bands at 340, 339 and 336 cm^{-1} are assigned to the individual out-of-plane deformation of C-N vibration and in-plane deformation of C-N vibration respectively.

Benzene and its derivatives generally show C–O stretching vibrations[23] in the region 1300-1100 cm^{-1}. The bands observed at 1565, 1322, 1266, 1110 cm^{-1} (FT-IR) and 1387, 1338, 1267, 1067 cm^{-1} (FT-Raman) may be assigned to C–O stretching of 5COMA. In this study stretching vibration due to C-O group attached with methyl group has been indentified at 1073cm^{-1} (strong FT-IR) and 1067cm^{-1} (strong FT-Raman) [23]. This mode can be described as vibrations involving main contributions from the C-O stretching vibrations.

The ring stretching vibrations[24] are usually at the region 1620–1390 cm^{-1}.The bands observed at 1646-1267 may be assigned to ring stretching vibrations.The substitution in ring implies many changes in vibrational modes of 5COMA. In the present study, the bands identified at 1073, 1071, 1067, 905, 903, 848, 846, 799, 788 and 779 cm^{-1} for 5COMA have been designated to ring in-plane and out-of-plane bending modes, respectively. The small change in frequencies observed for these modes are mainly due to the presence of methyl group in 5COMA and from varying extent of mixing between ring and constituent group vibrations.

Usually the N–H stretching vibrations[25] occur in the region 3500–3300 cm^{-1}. The stretching, scissoring and rocking deformation of the amino group appear at around 3500–3000, 1700–1600 and 1150–900 cm^{-1}, in the absorption spectra respectively[3]. For 5COMA, antisymmetric and symmetric stretching modes of NH_2 group were found at 3677, 3675, 3570, 3569 and 3568 cm^{-1}. The scissoring, rocking, wagging and twisting modes of the NH_2 group present in 5COMA were identified well within their characteristic regions. These modes are observed at 1692, 1690, 1689, 1476, 1472, 1110, 1073 cm^{-1} and 1650, 1338, 1134, 1067 cm^{-1} in FT-IR and FT-Raman respectively.

The C-Cl stretching gives strong bands in the 800–550 cm^{-1} region[26]. The sharp C-Cl stretching vibration has been observed in FT-IR and FT-Raman bands at 716, 712, 709 cm^{-1} and 660, 656, 587 cm^{-1} respectively.

Methyl group vibrations

For the assignments of CH_3 group frequencies, basically nine fundamentals can be associated to each CH_3 group, viz., CH_3 symmetric stretching (ss), CH_3 in-plane stretching (i.e., in-plane hydrogen stretching modes), CH_3 in-plane-bending (i.e., hydrogen deformation modes) CH_3 symmetric bending (sb), CH_3 in-plane rocking (ibr), CH_3 out-of-plane rocking(obr) and tCH_3 (twisting hydrogen bending modes). In addition, CH_3 ops, out-of-plane stretch and CH_3 opb, out-of-plane bending modes of the CH_3 group are expected to be depolarized for A' symmetry species[21]. The CH_3 ss frequency appears at 3088 and 3030 cm^{-1} in IR and CH_3 ips is observed at 3089 and 3087 cm^{-1} in FT-IR and FT-Raman, respectively for 5COMA. The symmetrical methyl deformation mode of CH_3 strong bending was observed at 1565, 1562, 1559 cm^{-1} in FT-IR. The bands at 3088, 3087, 3030, 3029 and 1525, 1523, 1192, 1190, 1188 cm^{-1} in FT-IR are attributed to CH_3 ops and CH_3 opb, respectively, in the $A^{'}$ species[27].

NMR chemical shift

The proton and carbon chemical shifts were calculated by the GIAO method using the B3LYP/ 6-311G** functional[21]. Experimental and calculated chemical shift values of ^1H and ^{13}C NMR spectroscopy are shown in Fig S1 (Supplementary Data). The chemical shift values obtained for 5COMA are listed in Table S3 (Supplementary Data). The chemical shift values for benzene derivatives are usually seen in the region higher than 100 ppm[28]. In the present study, ^{13}C NMR chemical shift values were higher than 100 ppm for 5COMA as also observed in earlier reports. The results of ^{13}C NMR indicates that the chemical shift values of methoxy group substituted carbon is greater than those of the amino group substituted carbon C1 and chlorine substituted carbon C5. This is due to greater electron negativity as well as greater deshielding effect (–O-CH3 > Cl > -NH2). This could be mainly due to inductive effect (greater electron negativity enhance the breaking of paramagnetic shielding character) of the substituted groups. The chemical shift values of C3, C4 and C6 carbons of the benzene ring are almost similar, but not for C5 carbon, which is due to inductive effect of Cl substituted in C5. The ^1H NMR chemical shift values of C3 and C4 protons are greater than that of the protons of C6 in benzene ring. The ^1H NMR chemical shift values of methoxy group protons are greater than the amino group protons.

Natural atomic charges

Natural atomic charges of a molecule can be obtained by quantum chemical calculations[29]. The atomic charges influence the electronic structure, dipole moment and other properties of molecules[30]. The results showed that the substitution of NH_2 and

OCH_3 groups modified the electron density of the aromatic ring. The C1 and C2 carbon atoms are highly positive and more acidic than C3, C4, C5 and C6. This may be attributed to the presence of $-NH_2$ and $-OCH_3$ in the respective carbons. The H11 and H12 hydrogen atoms and amino groups also have higher positive than hydrogen atom in C-H substitution. The charge distribution of 5COMA found by B3LYP functional is shown in Fig. S2 (Supplementary Data). The existence of negative charges on chlorine, nitrogen and oxygen atoms of 5COMA (Fig. S2) indicates that they are donors. Further, it can be seen from Fig. S2 that the negative charges of chlorine atom and the positive charges around hydrogen (greater positive charge of H11 proton from the benzene ring) atom wre combined to form the strong intra-molecular hydrogen bonding. The C1, C2 carbons are highly positive than C5 due the orientation effect (deactivating group of chlorine atom substituted in meta position of C5).

Molecular electrostatic potential (MEP)

MEP is used to predict the interaction of hydrogen bonding of the molecules. The molecular electrostatic potential electron density surface of 5COMA is shown in Fig. S2 (Supplementary Data). The electrophilic or nucleophilic nature of substituent groups and atoms of a molecule could be identified using MEP. The negative and positive surface of 5COMA is shown in different colour grades[21]. In MEP diagram, the electrophilic centre is given in red, whereas nucleophilic centre is in blue colour. The MEP diagram reveals the physicochemical properties viz., molecular size, shape, negative, positive and neutral electrostatic potential[31].

The negative regions are often associated with the lone pair of electronegative atom. From the results, it can be seen that the negative regions of 5COMA are nitrogen and oxygen, chlorine atoms, whereas positive charges lie on hydrogen atoms and ring systems. The MEP surface of 5COMA clearly reveals the formation of intra-molecular hydrogen bonding of chlorine atoms with nearby hydrogen (Cl12–H11) atom of ring.

NBO analysis

NBO analysis has been carried out to clarify the delocalization of charge due to the intra-molecular interaction between bonds, and for detailed information on conjugative interaction in molecular structure. The second-order perturbation theory has been investigated to explain the interacting stabilization energy from Lewis orbital and non Lewis orbital[16]. The higher E(2) value indicates more intensive interaction from occupied and unoccupied orbitals. The intra-molecular interaction are produced by the overlap among σ(C–C), π(C–C), σ*(C–C), π*(C–C) orbitals. These intra-molecular charge transfer (σ-σ*, π-π*) can encourage the nonlinearity of the molecule. The stabilization energy of bonding σ(C–C), π(C-C) to the antibonding σ*(C–C), π*(C-C) bond leads to stabilization of some part of the ring as is evident from Table 4. Since the NBO analysis gives the details on intra-molecular hydrogen bonding and stabilization energy, it plays a vital role in determining the electronic properties of a molecule[32]. Hence, it is concluded that the intra-molecular interaction has occurred through the orbital overlap of (C–C) bonding and (C–C) anti-bonding orbitals. The strong intra-molecular interaction of the σ electron of (Cl12) is distributed to π*(C4-C5), σ*(C5–C6), which leads to strong delocalization of the order of 41.75 kJ/mol.

Global and local reactivity descriptors

B3LYP/6-311G** method has been empolyed[33] to compute the chemical parameters, viz., molecular orbital (HOMO and LUMO) energies, energy gap (ΔE), electron affinity (EA), ionization potential (IP), hardness (η), dipole moment (μ), softness (S), absolute electronegativity (χ) and electrophilicity index (ω) (Supplementary Data, Table S4). The energies of HOMO and LUMO are related to the IP and EA, respectively in the framework of Koopmans' theorem .

$$\mathrm{IP} = -E_{\mathrm{HOMO}} \qquad \ldots(4)$$

$$\mathrm{EA} = -E_{\mathrm{LUMO}} \qquad \ldots(5)$$

The χ and η are determined from the IP and EA values.

$$\chi = \frac{\mathrm{IP+EA}}{2} \qquad \ldots(6)$$

S is defined as the inverse of the η (6). $S = \frac{1}{\eta}$, while the electrophilicity index (ω) is $\frac{\mu^2}{2\eta}$.

Table 4 – NBO analysis of 5COMA

Donor(I)	Occupancy	Acceptor (J)	Occupancy	E(2) (kcal/mol)	E(i)-E(j) (a.u.)	F(i,j)
σN10-C1	1.991	σ*C1-C2	0.02836	1.67	1.84	0.05
		π*C2-C3	0.02288	2.5	1.84	0.061
		σ*C5-C6	0.02238	2.26	1.83	0.058
σN10-H14	1.99389	π*C1-C6	0.01735	3.95	1.72	0.074
σN10-H15	1.99386	σ*C1-C2	0.02836	3.88	1.71	0.073
πC1-C6	1.97007	σ*C1-C2	0.02836	5.12	1.81	0.086
		σ*C5-Cl12	0.01988	5.3	1.32	0.075
σC2-O9	1.98864	σ*σC1-C2	0.02836	0.78	1.94	0.035
		π*C1-C6	0.01735	2.1	1.95	0.057
		σ*C13-H16	0.00876	2.19	1.75	0.055
πC4-C5	1.98047	σ*C4-H7	0.01085	1.76	1.64	0.048
		σ*C4-H7	0.01085	1.76	1.64	0.048
		σ*C5-C6	0.02238	5.45	1.81	0.089
		σ*C6-H11	0.01039	2.89	1.63	0.061
σC5-C6	1.97874	σ*N10-C1	0.01423	4.39	1.63	0.076
		π*C1-C6	0.01735	3.96	1.83	0.076
		π*C4-C5	0.02386	5.37	1.81	0.088
σC5-CL12	1.98952	π*C1-C6	0.01735	3.02	1.78	0.066
		σ*C3-C4	0.01384	2.91	1.78	0.064
σC6-H11	1.98017	σ*C1-C2	0.02836	5.49	1.56	0.083
		σ*C4-C5	0.02386	4.64	1.55	0.076
N10(LP)	1.89026	π*C1-C6	0.37548	38.96	0.56	0.142
		π*C2-C3	0.36312	0.51	0.56	0.016
O9(LP)	1.96728	σ*N10-H14	0.00417	0.57	1.52	0.026
		π*C2-C3	0.02288	5.7	1.64	0.087
		σ*C3-C4	0.36312	2.28	0.96	0.046
		σ*C13-H17	0.01579	3.57	1.43	0.064
CL12(LP)	1.99416	π*C4-C5	0.02386	41.75	2	0.053
		σ*C5-C6	0.02238	41.75	2	0.053

The electrophilicity (ω) is a significant parameter which is the measure of the molecule to accept the electrons. Nucleophilicity (ε) is an index of the molecule to donate the electrons (1/ω). Thus, the electrophilicity and nucleophilicity of a molecule influence the electronic property of a molecule. The molecule with higher electrophilicity values will be a poor donor whereas the molecule having higher nucleophilicity will function as good donor. Thus, the reactivity of molecules and atoms are directly related to the ionization potential. But the softness and hardness of molecules give information about stability in addition to the reactivity. The observation of higher softness values for 5COMA, categorized it as highly reactive, stable and soft molecule.

First-order hyperpolarizability and polarizability calculations

The Kleinman symmetry of 3D matrix molecule has been decreased to 10 components, and provides the lower tetrahedral format[34]. The vibrational spectroscopy analyse reveal that 5COMA had conjugated electrons, thus showing the higher values of first-order hyperpolarizability. The highest value of β is related to the non linear optical behaviour of the molecules, and correlated with the intra-molecular charge transfer[35] (ICT). This is due to the movement of electron donor-electron acceptor groups with the conjugated π systems[35]. The value of first-order hyperpolarizability (β_{total}) of 5COMA is 1.6179×10^{-30} esu; it is almost 8 times larger than that of urea (0.1947×10^{-30} esu).

The polarizability of the molecule is isotropic if all the polarizabilities lie in the same direction with spherical symmetry of electron density. Otherwise, it is said to be anisotropic if the direction of polarizability is not the same. Polarizability of a molecule often related to Raman scattering. The isotropic polarizability and the anisotropy polarizability invariant calculated with the arithmetical derivative of the dipole moment using B3LYP/6-311+G** are shown in Table S5 (Supplementary Data). The isotropic polarizability ($\bar{\alpha}$) is given by

$$\bar{\alpha} = 1/3(\alpha_{xx} + \alpha_{yy} + \alpha_{zz}).$$

The anisotropy polarizability invariant is given by

$$\gamma^2 = 1/2\begin{bmatrix}(\alpha_{xx}-\alpha_{yy})^2\\+(\alpha_{yy}-\alpha_{zz})^2\\+(\alpha_{zz}-\alpha_{xx})^2\\+6(\alpha^2_{xy}+\alpha^2_{yz}+\alpha^2_{zx})\end{bmatrix} \quad \ldots(8)$$

The average hyperpolarizability is

$$\beta_{\text{total}} = (\beta^2_x + \beta^2_y + \beta^2_z)^{1/2} \quad \ldots(9)$$

Hence, α_{xx}, $\alpha_{yy,}$ and α_{zz} are tensor components of polarizability, whileβ_x, β_y and and β_z are tensor components of hyperpolarizability.

NLO activity

The theoretically calculated hyperpolarizability shows the relationship between the molecular structure and NLO activity. The first-order hyperpolarizability value (β_{total}) of 5COMA is 1.6179×10^{-30} esu, which is larger than that of urea (0.1947×10^{-30} esu). The higher β values obtained for 5COMA reveal the NLO property of the molecule. The lower HOMO-LUMO energy gap indicates that charge transfer interaction takes place within the molecules[36]. The molecular orbital of HOMO and LUMO of 5COMA are shown in Fig. S4 (Supplementary Data). The frontier molecular orbitals of 5COMA indicates NLO properties, greater hyperpolarizability and lower HOMO–LUMO energy gap. The intra-molecular charge transfer is due to the overlapping of lone pair electrons of chlorine (Cl12) with hydrogen (H11) atom of phenyl ring.

Electronic excitation mechanism

static polarizability value is directly proportional to the optical intensity and inversely related to the cube of transition energy[21]. With this concept, larger oscillator strength (f_n) and $\Delta\mu_{gn}$ with lower transition energy (E_{gn}) is favourable to obtain large first static polarizability values. Electronic excitation energies, oscillator strength and characteristics of the respective excited states were calculated by the closed-shell singlet calculation method is shown in Table S6 (Supplementary Data). Representation of the orbital involved in the electronic transition for FMO is shown in Fig. S5 (Supplementary Data).

Conclusions

The structure of 5COMA in complete optimization mode confirmed the Cs point group symmetry. The vibrational spectroscopic analyses of 5COMA clearly indicated the number of NOC as 48. Further, bonding nature of atoms in a molecule has been evaluated using FT-IR and FT-Raman spectral analyses. The formation of intra-molecular hydrogen bonding has been confirmed by NAC of 5COMA. MEP of the compound revealed the electrophilic and nucleophilic reactivity. The stability, reactivity and softness of the molecule have been known by global and local reactivity description of 5COMA. The structural features of the molecule have been confirmed using ^{1}H and ^{13}C NMR spectral data. The intra-molecular hydrogen bonding of the studied molecule was further shown by NBO analysis. The NLO property has been confirmed by first order hyperpolarizability values of 5COMA. Further, HOMO-LUMO energy values support the NLO activity of 5COMA.

Supplementary Data

Supplementary Data associated with this article, i. e., Figs S1-S5 and Tables S1-S6, are available in the electronic form at http://www.niscair.res.in/jinfo/ijca/IJCA_55A(04)413-422_SupplData.pdf.

References

1 Vaschetto E, Retamal B A & Monkman A P, *J Mol Struct (Theochem),* 468 (1999) 209.
2 Green J H S, Harrison D J & Stockley C P, *Spectrochim Acta A*, 33 (1977) 423.
3 Sivaranjini T, Periandy S, Govindarajan M, Karabacak M & Asiri A M, *J Mol Struct,*1056 (2014) 176.
4 Kolandaivel P, Praveena G & Selvarengan P, *J Chem Sci,* 117 (2005) 591.
5 Usha Rani A, Sundaraganesan N, Kurt M, Cinar M & Karabacak M, *Spectrochim Acta,* 75 (2010) 1523.
6 Karabacak M, Kurt M & Atac A, *J Phys Org Chem,* 22 (2009) 321.
7 Ramalingam S, Periandy S, Narayanan B & Mohan S, *Spectrochim Acta,* 76 (2010) 84.
8 Karabacak M, Karagoz D & Kurt M, *Spectrochim Acta A,* 72 (2009) 1076.
9 *Gaussian 03 Program, Gaussian Inc, Wallingford CT*, 2004.
10 Becke A D, *J Chem Phys*, 98 (1993) 5648.
11 Lee C, Yang W & Parr R G, *Phys Rev B,* 37 (1998) 785.
12 Sundius T, *Vib Spectrosc,* 29 (2002) 89.
13 Sundius T, *J Mol Struct,* 218 (1990) 321.
14 Reed A M, Curtiss L A & Weinhold F, *Chem Rev,* 88 (1988) 899.
15 James C, Amal Raj A , Reghunathan R, Hubert Joe I & Jayakumar V S, *J Raman Spectros,* 37 (2006) 1381.
16 Jagadeesan R, Velmurugan G & Venuvanalingam P, *RSC Adv, 5* (2015) 80661.

17 Sebastian S & Sundaraganesan N, *Spectrochim Acta: A,* 75 (2010) 941.
18 Fogarasi G, Pulay P, & J R Durig (Ed.), Vibrational Spectra and Structure, *Elesevier Amsterdam*, 14 (1985) 125.
19 Fogarasi G, Zhov X, Taylor P W & Pulay P, *J Am Chem Soc,* 114 (1992) 8191.
20 *Application of Electronic Structure Theory, Modern Theoretical Chemistry,* Vol. 4, edited by P Pulay & Schaefer H F III, (Plenum Press) 1997, p. 153.
21 Vennila P, Govidaraju M, Venkatesh G & Kamal C, *J Mol Struct,* 1111 (2016) 151.
22 Krishnakumar V & John Xavier R, *Indian J Pure Appl Phys,* 41 (2003) 597.
23 Krishnakumar V & Balachandran V, *Indian J Pure Appl Phys,* (2004) 313.
24 Karabacak M, Cinar M, Unal Z & Kurt M, *J Mol Struct,* 982 (2010) 22.
25 Altun A, Golcuk K & M. Kumru, *J Mol Struct (Theochem)*, 625 (2003) 17.
26 Fu A, Du D & Zhou Z, *Spectrochim Acta A,* 59 (2003) 245.
27 Venkatesh G, Govindaraju M & Vennila P, *Asian J Chem*, 28 (2016) 675.
28 *Infrared and Raman Characteristic Group Wave numbers, Tables and Charts,* III EDITED BY George S, (Wiley, Chichester) 2001.
29 Osmialoswski B, Kolehmainen E & Gawinecki R, *Magn Reson Chem,* 39 (2001) 334.
30 Sidir I, Sidir Y G, Kumalar M & Tasal E, *J Mol Struct,* 964 (2010) 134.
31 Luque F J, Orozco M, Bhadane P K & Gadre S R, *J Phys Chem*, 97 (1993) 9380.
32 Venkatesh G, Govindaraju M, Vennila P & Kamal C, *J Theor Comput Chem*, 15 (2016) 1650007.
33 Vedha S A, Velmurugan G, Jagadeesan R & Venuvanalingam P, *Phys Chem Chem Phys,* 17 (2015) 20677.
34 Kaya S & Kaya C, *Comput Theor Chem*, 1052 (2015) 42.
35 Nagarajan N, Velmurugan G, Venuvanalingam P & Renganathan R, *J Photochem Photobiol A Chem,* 284 (2014) 36.
36 Nagarajan N, Velmurugan G, Prakash A, Shakti N, Katiyar M, Ponnambalam Venuvanalingam P & Renganathan R, *Chem Asian J*, 9 (2014) 294.